Chen *et al. Journal of Ovarian Research* (2024) 17:252
https://doi.org/10.1186/s13048-024-01578-y

Journal of Ovarian Research

RESEARCH Open Access

TIGIT$^+$ CD4$^+$ regulatory T cells enhance PD-1 expression on CD8$^+$ T cells and promote tumor growth in a murine ovarian cancer model

Fengzhen Chen[1*], Yanying Xu[1], Xiangyu Liu[2], Na Dong[1] and Lei Tian[3]

Abstract
Immune checkpoint-based immunotherapy has shown limited efficacy in the treatment of ovarian cancer. In recent years, the emergence of immune checkpoint co-targeting therapies, led by the combination targeting of TIGIT and FAK, has shown promise in ovarian cancer treatment. Our preliminary research indicates that TIGIT is predominantly expressed in regulatory T cells during ovarian cancer. However, the therapeutic impact of TIGIT targeting based on regulatory T cells in ovarian cancer remains to be elucidated. We utilized ID8 cells to establish a mouse model of ovarian cancer. Through flow cytometry and co-culture methods, we validated the relationship between the functionality of regulatory T cells and tumor masses, and confirmed the crucial role of TIGIT in immune suppression in ovarian cancer. Furthermore, using Foxp3-diphtheria toxin receptor (DTR) mice, we substantiated that the combined TIGIT antibody treatment, based on targeting regulatory T cells, effectively slowed down the progression of ovarian cancer. Taken together, our results have demonstrated that dual targeting of regulatory T cells and TIGIT effectively retards tumor growth, laying the groundwork for the clinical application of immune checkpoint combination therapies. Future research in ovarian cancer immunotherapy is leaning towards a strategy that combines multiple targets, and specific cell-type immunotherapies.

Keywords TIGIT, Ovarian cancer, Regulatory T cell, PD-1

Introduction

Ovarian cancer has an incidence of approximately 20,000 new cases annually in the USA and is the most lethal of the gynecologic malignancies. Despite other cancers such as endometrial cancer having higher rates of incidence, ovarian cancer mortality rates continue to be high [1]. It is a heterogeneous disease comprising distinct subtypes, the most common being high-grade serous ovarian cancer (HGSOC). Due to the limited frequency of screening and non-specific symptoms, most cases (>80%) of HGSOC are diagnosed at an advanced stage (International Federation of Gynecology and Obstetrics stage III and IV) when tumor has spread to the peritoneal cavity

*Correspondence:
Fengzhen Chen
cfz_blue_7@163.com
[1]Department of Gynecology, The Second Hospital of Tianjin Medical University, Tianjin 300211, China
[2]Tianjin Medical University Cancer Institute and Hospital, Tianjin 300060, China
[3]Department of Gynecology and Obstetrics, The Affiliated Hospital of Nankai University, Tianjin No. 4 Hospital, Tianjin 300222, China

and upper abdominal organs [2]. The 5-year survival rate of HGSOC is below 50%. The current standard therapy is debulking surgery and platinum-based chemotherapy, which is limited by the frequent development of chemoresistance [3–5].

Immunotherapy stands as a pivotal cornerstone in the comprehensive treatment approach for HGSOC. While initial reports had suggested limited effectiveness of immunotherapy, primarily due to the scarce presence of immune cells, recent years have witnessed a multitude of promising immunotherapy studies [6–8]. The capacity of cancer cells to evade the immune system poses a significant barrier to immunotherapeutic interventions [9]. The infiltrative migration of suppressive regulatory T cells into HGSOC tissue profoundly influences the prognosis of this malignancy [10]. Research has uncovered a substantial accumulation of $CD4^+CD25^+$ regulatory T cells (Tregs) in the bloodstream, lymph nodes, and tumor sites of individuals diagnosed with ovarian cancer, with this heightened presence of Tregs negatively correlated with the overall prognosis of patients, indicating a substantial compromise in their immune functionality [11–14]. However, studies have revealed that therapeutic interventions specifically targeting Tregs have not resulted in discernible clinical benefits [15], and the factors contributing to this phenomenon remain elusive.

The T-cell immunoglobulin and ITIM domain (TIGIT), a recent addition to the CD28 family, was computationally identified by three distinct research groups back in 2009. This receptor is expressed on activated conventional αβ T cells, as well as on memory T cells, regulatory T cells, follicular helper cells, and NKT cells [16]. A study revealed that in ovarian cancer patients who experience recurrence after chemotherapy, there was an elevation in the levels of TIGIT and CTLA4 in the tumor tissue [17]. In the context of ovarian cancer mouse models, our research team has demonstrated that TIGIT is predominantly expressed on $CD4^+$ Tregs and was closely linked to the prognostic outcomes in mice afflicted with ovarian cancer [18]. Although numerous studies have confirmed the ineffectiveness of immune therapy solely targeting TIGIT in ovarian cancer, a multi-targeted immune approach involving TIGIT may prove efficacious. For instance, recent findings indicate that the combination of TIGIT and focal adhesion kinase (FAK) can enhance the survival rate in HGSOC [19]. Therefore, a predominantly TIGIT-focused combination targeted therapy, including Tregs targeting, may contribute to advancing immunotherapy for ovarian cancer.

However, the precise mechanisms through which $TIGIT^+CD4^+$ Tregs impact the immune processes and therapeutic outcomes in ovarian cancer remain to be elucidated. We postulate that $TIGIT^+CD4^+$ Tregs may occupy a pivotal role in shaping the trajectory of ovarian cancer progression and the intricate mechanisms governing the anti-tumor activities of $CD8^+$T cells. Based on the above, we sought to elucidate the role of $TIGIT^+CD4^+$ Tregs in ovarian cancer and assess the potential efficacy of immunotherapy targeting these cells in the treatment of HGSOC.

Materials and methods

Study animals

Female C57BL/6 mice (6–8 weeks old) were purchased from the Laboratory Animal Center of the Chinese Academy of Medical Sciences and housed in well-ventilated cabinets under standard environmental conditions (temperature 21±2 °C, 50-60% relative humidity, and a conventional 12/12 h light/dark cycle). DEREG mice (C57BL/6 background, MMRRC Stock No: 32050-JAX) were purchased from The Jackson Laboratories (USA). The use of animals was ethically approved by the Tianjin Medical University ethics committee. Mice (8–10 mice/group) received intraperitoneal injections of 1×10^6 ID8 cells 10 days before initiating treatments. Ovarian cancer mice underwent three intraperitoneal injections at 4-day intervals with 100 μg of control (Ultra-LEAF™ Purified Mouse IgG1, κ Isotype Ctrl Antibody, Catalog#401414, BioLegend) or anti-TIGIT monoclonal antibody (Clone 1B4, Catalog#Ab01258, Absolute Antibody Ltd.) [20] following the same method as in our previous research [18]. Seven days later, spleens and ascites from treated mice were harvested, and mononuclear cells were isolated and analyzed by flow cytometry.

For survival experiments, mice (20 mice/group) received intraperitoneal injections of 1×10^6 ID8 cells 10 days before treatment. In the treatment groups, mice were administered three doses of 100 μg of control or anti-TIGIT monoclonal antibody at 4-day intervals. Mice were weighed bi-weekly, and daily observations were made for signs of swollen bellies indicative of ascites formation. Additionally, evidence of toxicity, such as weight loss, hunched posture, mobility, diarrhea, failure to eat, and respiratory distress, was assessed daily. Mice were euthanized upon the development of ascites and a weight increase exceeding 30%, following institutional guidelines. The mean survival time of mice was calculated using the Kaplan-Meier survival curve and log-rank test.

Tregs depletion

To deplete Tregs, we utilized DEREG mice, which express DTR under the control of the Foxp3 promoter (Foxp3-DTR mice). As previously described in detail [21], these mice were administered an intraperitoneal injection of 1 μg DT (Catalog #322326, Merck) or PBS 24 h before 1×10^6 ID8 cells injection. Subsequently, 1 μg DT was administered on day 7 following tumor implantation.

Control mice were treated with PBS injection. Flow cytometry in blood were used to confirm Tregs depletion.

Tumor volume measurement

To remove bias, a blind tumor volume measurement was done. Tumor volume was calculated using the following formula [22]: Tumor volume (mm3) = ($L \times W^2$) / 2. "L" and "W" represented the longest and shortest diameter of the tumor, respectively.

Cell lines

ID8, a well-established clone of the MOSEC ovarian cancer derived from C57BL/6 mice (Catalog #SCC145), was generously provided by the University of Pennsylvania. Prior to cell suspension preparation and subsequent administration to mice, ID8 cells underwent cultivation under controlled conditions at 37 °C in an atmosphere of 5% CO_2. This cultivation process occurred in a complete DMEM medium, enriched with essential components, including 10% Fetal Bovine Serum (FBS) (Catalog #10099, Gibco), 100 U/mL of penicillin, and 100 µg/mL of streptomycin.

Antibodies and flow cytometry analysis

Flow cytometry analyses were conducted on multiple occasions, up to three times, to comprehensively characterize the phenotypes of immune cells present in both the spleen and ascites. A panel of monoclonal antibodies, including CD3 PerCP (Clone SK7, Catalog #145-2C11, BD Biosciences), CD4 Pacific Orange (Clone RM4-5, Catalog #MCD0430, Invitrogen), CD8 Pacific Blue (Clone SK1, Catalog #344718, BioLegend), CD25 PE-Cy7 (Clone PC61, Catalog #552880, BD Biosciences), PD-1 FITC (Clone 29 F.1A12, Catalog #135214, BioLegend), FoxP3 PE (Clone MF23, Catalog #560408, BD Biosciences), and TIGIT BV605 (Clone 1G9, Catalog #744212, BD Biosciences), were thoughtfully selected for immune cell staining.

To perform these analyses, mononuclear cells (1.5×10^6 cells) isolated from both the spleen and ascites were incubated with prepared antibody mixtures using FACS buffer, composed of PBS with 2% BSA and 0.05% sodium azide, at a dilution of 1:100. This incubation occurred for 15 min at a controlled temperature of 4 °C, followed by two thorough washes. Subsequently, for intracellular staining of FoxP3 following the manufacturer's instructions, the cells were fixed and permeabilized using a BD Cytofix/Cytoperm kit (Catalog #554714, BD Biosciences).

Following the staining and preparation steps, the cells were promptly analyzed using a BD LSR II multicolor flow cytometer (BD Biosciences). The acquired data underwent in-depth analysis using FlowJo software version 10, developed by Tree Star.

Isolation of splenic CD4+CD25+ Tregs and CD4+CD25− T effector cells

Spleens were harvested and processed into a single-cell suspension by passing through 40 µm filters twice. Mononuclear cells were then isolated using Ficoll-Paque density gradient centrifugation. $CD4^+CD25^+$ Tregs and $CD4^+CD25^-$ T effector cells were isolated utilizing a mouse $CD4^+CD25^+$ Tregs isolation kit (Catalog #130-091-041, Miltenyi Biotec) [23]. The purity of T cells was estimated to be >90% by FACS. The isolated cells were cultured in RPMI 1640 supplemented with 10% FBS.

Coculture

Splenic $CD4^+$ Tregs were isolated from both untreated normal mice and ovarian cancer mice, including those in the isotype control and anti-TIGIT treatment groups. Subsequently, they were co-cultured with normal splenic $CD4^+CD25^-$ T effector cells from untreated normal mice for a period of 24 h, maintaining a ratio of 1:1 (2×10^5 cells/well). The co-cultures were then subjected to treatment with anti-CD3 (5µg/ml) and anti-CD28 (2 µg/ml) for the polyclonal activation of T cells following the same method as in our previous research [18]. The proliferation and apoptotic rate of $CD4^+CD25^-$ T effector cells were assessed using CCK-8 and Annexin-V Staining, while the secretory capacity (IFN-γ and IL-4) was determined via ELISA.

CCK-8 measurement

Splenic $CD4^+CD25^-$ T effector cells from untreated normal mice and splenic $CD4^+$ Tregs, obtained from untreated normal mice, as well as from ovarian cancer mice in the isotype control and anti-TIGIT treatment groups, were co-cultured at a 1:1 ratio. Following a 24-hour co-culture, cells in the supernatant were gathered and distributed to 96-well plates in triplicate, with a seeding density of 1×10^5 cells per well. Subsequently, 10 µl of CCK-8 (Dojindo Molecular Technologies, Inc., Kumamoto, Japan) was introduced to each well, and the cells were incubated for 4 h at 37 °C in the absence of light exposure. Absorbance was measured using a microplate reader (Spectra MR, Dynex, Richfield, MN) at OD450nm.

Annexin-V staining

Cell apoptosis was assessed using the Annexin V-fluorescein isothiocyanate apoptosis kit (Nanjing Keygen Biotech, Nanjing, China) in accordance with the manufacturer's instructions. In brief, cells were resuspended in 100 µl of binding buffer containing 5 µl of Annexin-V and 5 µl of 7-AAD, followed by a 15-minute incubation at room temperature. Afterward, the cells were washed twice with cold PBS. Subsequently, cells were diluted by adding 300 µl of binding buffer and promptly analyzed

using flow cytometry within 1 h. The data are presented as the percentage of Annexin-V-positive cells.

ELISA

The supernatants obtained from the co-culture were collected for the quantification of IFN-γ and IL-4 levels using ELISA kits (Catalog #BMS606, #BMS613, Invitrogen). The procedure strictly adhered to the protocols provided by the manufacturer. In summary, the supernatants were diluted 1:1 with sample dilution buffer, and 100 µl of each sample was added to the respective wells. For the calibration curve, a dilution series of the standard was prepared on the same plate. The plate was incubated at 37 °C for 1 h. Following this, the samples were removed, and the wells were washed five times with the washing solution. An enzyme-labeled secondary antibody, diluted with sample dilution buffer, was added (100 µl per well) and incubated at 37 °C for 1 h. After the reaction, the secondary antibody was removed, and the wells were washed five times with the washing solution. A substrate solution was added, and the color developed during incubation. Upon sufficient color development, a stop solution was added, and the absorption at 450 nm was measured using a plate reader (Spectra MR, Dynex).

Statistics

Statistical analyses were performed using GraphPad Prism V9.0 (GraphPad Software, La Jolla, California, USA). The data shown are representative of three independent experiments. Continuous variables in figures are expressed as the mean ± SEM. The Mann-Whitney test, univariate analysis of variance (ANOVA, Least Significant Difference test), and Student t-test were two-tailed and employed to calculate P values. A significance level of $P<0.05$ was considered statistically significant.

Results

TIGIT+Foxp3+CD4+ T cells exhibited a notable increase in ovarian cancer mice

The examination of TIGIT expression on both $CD4^+Foxp3^+$ and $CD4^+Foxp3^-$ T cell populations in ovarian cancer mice involved the collection of mononuclear cells from the spleen and ascites, a week after establishing the ovarian cancer model. Subsequent staining and flow cytometry analysis revealed that within ovarian cancer mice, the $TIGIT^+Foxp3^+CD4^+$ T cell subset demonstrated a significant elevation compared to normal mice. This increase was evident in both spleen lymphocytes (4.497 ± 0.692% vs. 1.123 ± 0.251%, $P<0.01$) and ascites (13.033 ± 1.377% vs. 4.615 ± 1.099%, $P<0.01$; Fig. 1).

The immunosuppressive capacity of TIGIT+CD4+ Tregs was found to surpass that of TIGIT−CD4+ Tregs

To validate the immunosuppressive function of $TIGIT^+CD4^+$ Tregs, we established co-cultures involving effector T cells ($CD4^+CD25^-$ T cells) and either $TIGIT^+CD4^+$ or $TIGIT^-CD4^+$ Tregs. For this investigation, ovarian cancer mice induced by ID8 cells were sacrificed ten days after the injection of ID8 cells. We isolated splenic $TIGIT^+CD4^+Foxp3^+$ Tregs and $TIGIT^-CD4^+Foxp3^+$ Tregs, which were subsequently co-cultured with normal effector T cells ($CD4^+CD25^-$ T cells) sourced from healthy mice. The co-cultures were stimulated with anti-CD3 and anti-CD28.

We found that the proliferation of effector T cells was significantly suppressed in the $TIGIT^+CD4^+$ Tregs group compared to the $TIGIT^-CD4^+$ Tregs group (0.578 ± 0.068 vs. 0.416 ± 0.048, $p<0.01$). Additionally, apoptosis rates were elevated (46.25 ± 2.513 vs. 58.38 ± 3.210, $p<0.01$) in the $TIGIT^+CD4^+$ Tregs group compared to the $TIGIT^-CD4^+$ Tregs group. Furthermore, the secretory functions of effector T cells, measured through the production of IFN-γ (99.82 ± 6.983 pg/ml vs. 72.17 ± 3.769 pg/ml, $p<0.01$) and IL-4 (192.8 ± 5.544 pg/ml vs. 126.8 ± 8.804 pg/ml, $p<0.01$), were notably reduced by $TIGIT^+CD4^+$ Tregs in comparison to the $TIGIT^-CD4^+$ Tregs group (see Fig. 2).

The augmentation of TIGIT+Foxp3+ T cells occurred concomitantly with PD-1 expression on CD8+ T cells during tumor growth

To explore the influence of $TIGIT^+Foxp3^+$ Tregs in increasing the PD-1 expression on $CD8^+$ T cells, we conducted a kinetic analysis tracking the infiltration of tumor-associated $TIGIT^+Foxp3^+$ Tregs alongside the appearance of exhausted $TIGIT^+PD\text{-}1^+CD8^+$ T cells during the progression of ovarian cancer. Our observations unveiled a clear correlation between the accumulation of $TIGIT^+Foxp3^+$ Tregs and the growth of ovarian cancer tumors ($r^2=0.9258$, $p<0.0001$), while the levels of $TIGIT^-Foxp3^+$ Tregs displayed a decreasing trend in parallel ($r^2=0.9258$, $p<0.0001$) (see Fig. 3A). Furthermore, we noted that $TIGIT^+PD\text{-}1^+CD8^+$ T cells exhibited a steady accumulation as tumor growth progressed ($r^2=0.9380$, $p<0.0001$). In contrast, the ratio of $TIGIT^-PD\text{-}1^+CD8^+$ T cells ($r^2=0.2399$, $p=0.106$) and $TIGIT^-PD\text{-}1^-CD8^+$ T cells ($r^2=0.0528$, $p=0.4726$) did not exhibit significant changes in response to tumor growth (see Fig. 3B). Taken together, the increased presence of $TIGIT^+Foxp3^+$ Tregs paralleled the expression of PD-1 on $CD8^+$ T cells during tumor growth.

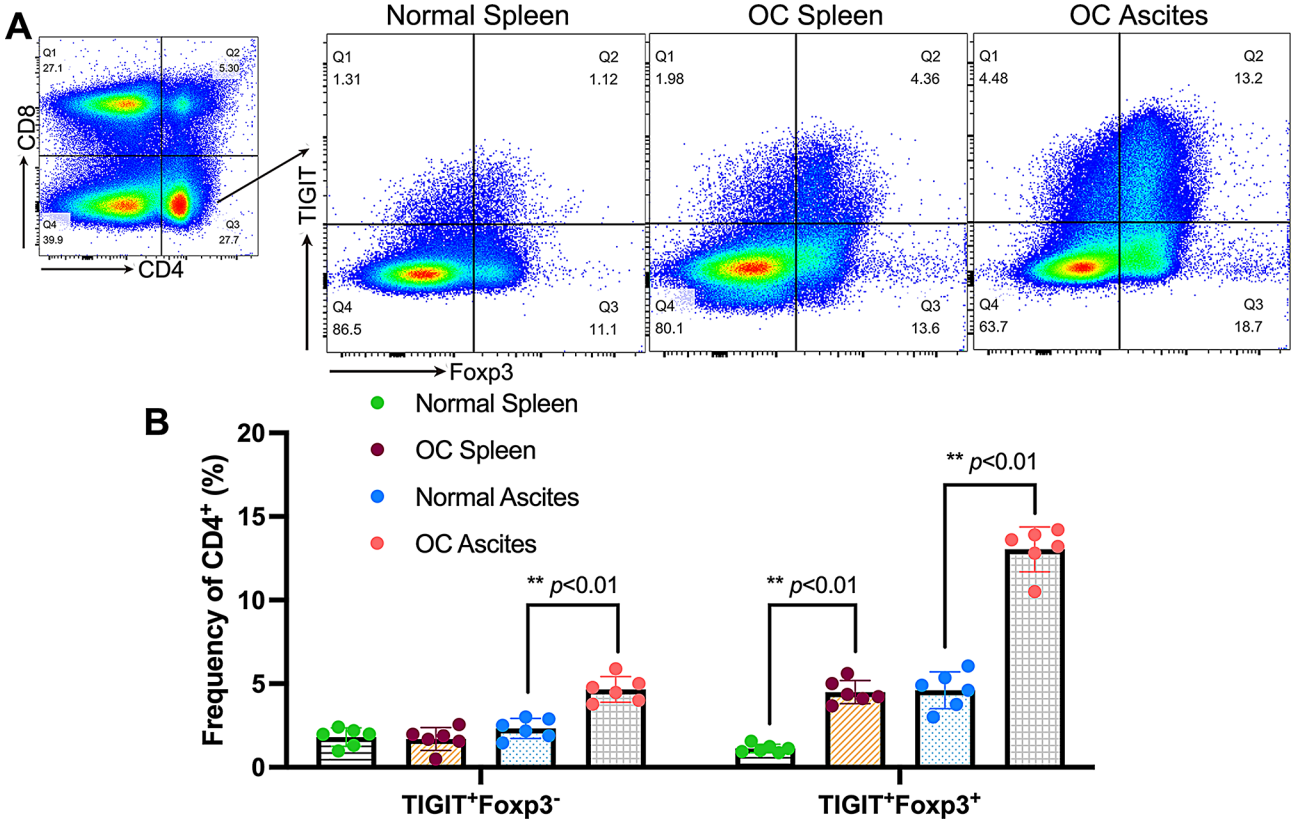

Fig. 1 The evaluation of TIGIT expression on both Foxp3$^-$CD4$^+$ and Foxp3$^+$CD4$^+$ T cell populations was undertaken. In a cohort of mice ($n=6$), each receiving an i.p. injection of 1×10^6 ID8 cells, peritoneal lavage fluid and spleen samples were collected seven days post-injection from both ovarian cancer and normal mice ($n=6$). Mononuclear cells were isolated via Ficoll-Paque density gradient centrifugation. Flow cytometry was utilized to assess the proportions of TIGIT$^+$Foxp3$^+$CD4$^+$ and TIGIT$^+$Foxp3$^-$CD4$^+$ lymphocytes within the spleen and ascites (A). Additionally, the frequency of TIGIT$^+$ cells within Foxp3$^+$ and Foxp3$^-$ CD4$^+$ T cell subpopulations found in the spleen and ascites was examined (B). The results are depicted as means ± standard deviation. OC, ovarian cancer

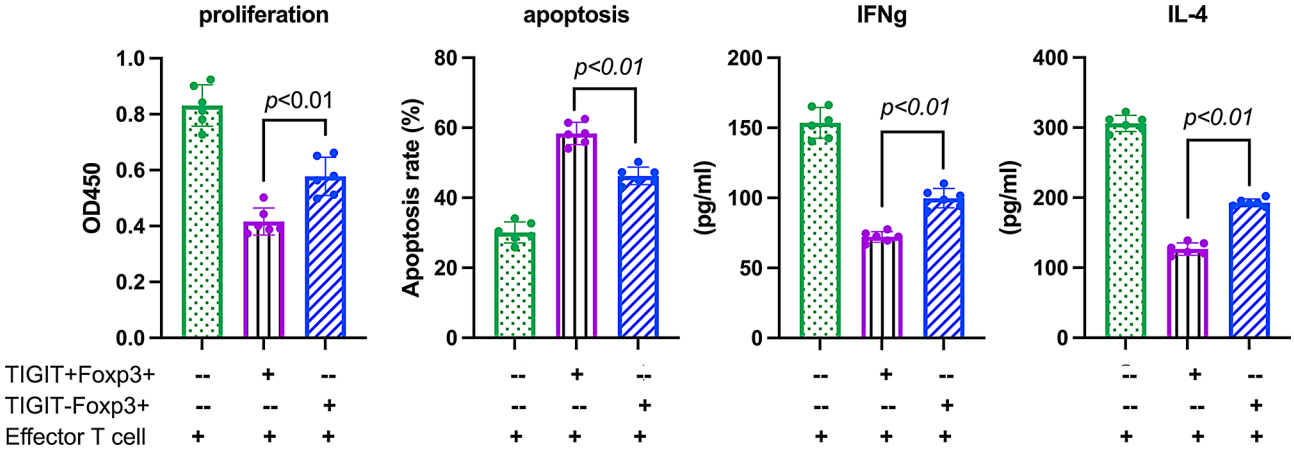

Fig. 2 Enhanced Immunosuppression by TIGIT$^+$CD4$^+$Tregs Compared to TIGIT$^-$CD4$^+$Tregs. Groups of mice (six individuals per group) were subjected to i.p. injection with 1×10^6 ID8 cells. Ten days following injection, splenic TIGIT$^+$CD4$^+$Foxp3$^+$ Tregs and TIGIT$^-$CD4$^+$Foxp3$^+$ Tregs were isolated through flow sorting techniques from various experimental groups. These isolated cells were subsequently co-cultured with normal effector T cells (CD4$^+$CD25$^-$ T cells) sourced from healthy mice. The co-cultures were stimulated with anti-CD3 (5 μg/mL) and anti-CD28 (2 μg/mL) at a 1:1 ratio for a duration of 24 h. Proliferation (**A**), apoptotic rate (**B**), and the secretory potential (IFN-γ and IL-4) (C and D) of CD4$^+$CD25$^-$ T cells were assessed and quantified. The results are represented as means ± standard deviation

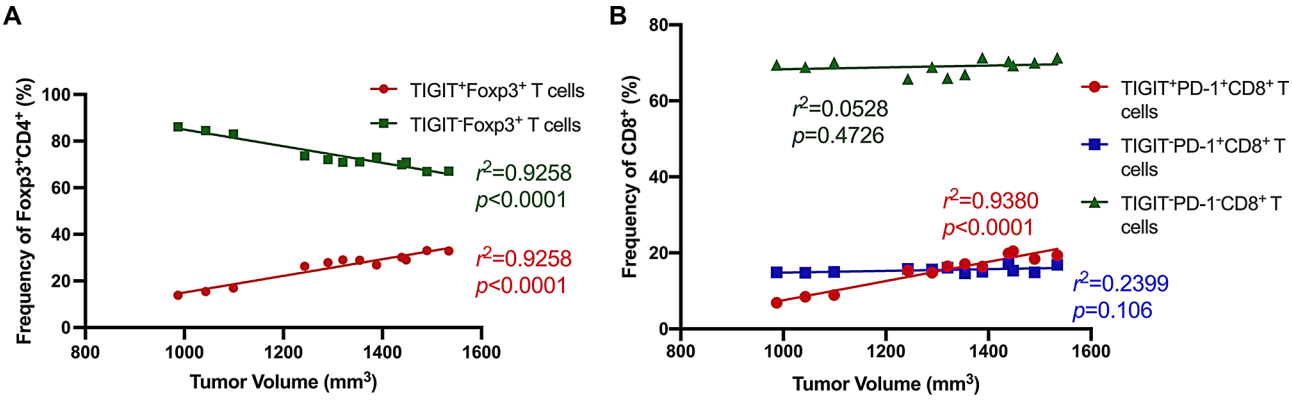

Fig. 3 Profiling Tumor-Infiltrating Lymphocytes in ovarian cancer Mice Over Time. Tumor-infiltrating lymphocytes were harvested from ovarian cancer mice induced by ID8 cells at distinct time points following implantation and subsequently analyzed using flow cytometry. On the 10th ($n=3$), 15th ($n=3$), 20th ($n=3$), and 25th ($n=3$) days post-modeling, tumor volumes were measured. (**A**) The figure illustrates the frequency of $TIGIT^+$ and $TIGIT^-$ cells within the $Foxp3^+CD4^+$ T cell population in tumor-infiltrating lymphocytes. The r^2 values for $TIGIT^+$ and $TIGIT^-$ Tregs are 0.9258 and 0.9258, respectively. (**B**) The panel showcases the frequency of different subpopulations among $CD8^+$ tumor-infiltrating lymphocytes expressing TIGIT and PD-1. Specifically, for $CD8^+TIGIT^+PD\text{-}1^+$ T cells, the r^2 is 0.9380; for $CD8^+TIGIT^-PD\text{-}1^+$ T cells, the r^2 is 0.2389, and for $CD8^+TIGIT^-PD\text{-}1^-$ T cells, the r^2 is 0.4726

Foxp3+ Tregs depletion decreased the PD-1 expression on CD8+ T cells

To substantiate the hypothesis implicating a substantial role for $TIGIT^+$ $CD4^+$Tregs in the development of a dysfunctional phenotype in $CD8^+$ T cells, we introduced diphtheria toxin (DT) to mice that featured stable expression of the DT receptor under the Foxp3 promoter's control (Foxp3-DTR mice) seven days post-tumor implantation. On day 14 following DT or PBS injection, we sacrificed tumor-bearing mice that had received either PBS or DT treatment. First, we confirmed that the depletion of Tregs met the efficiency criteria by analyzing blood samples from the mice using flow cytometry (Supplementary Fig. 1). We found that after using DT to deplete regulatory T cells, the frequency of $CD8^+TIGIT^+PD\text{-}1^+$ T cells (9.248 ± 1.518 vs. 20.52 ± 1.439, $p<0.01$) and $CD8^+TIGIT^-PD\text{-}1^+$ T cells (8.482 ± 0.6521 vs. 19.95 ± 1.583, $p<0.01$) in ovarian tumor microenvironment was significantly reduced (see Fig. 4A and B). Furthermore, we undertook kinetic assessments tracking the growth of ovarian cancer tumors following the depletion of $Foxp3^+$ Tregs. These investigations demonstrated that Tregs depletion led to a significant retardation in ovarian cancer tumor growth (see Fig. 4C).

The inhibition of tumor growth by anti-TIGIT treatment hinges on Foxp3+ Tregs

To explore the potential synergistic impacts arising from anti-TIGIT treatment and the depletion of $Foxp3^+$ Tregs on tumor growth inhibition, we harnessed Foxp3-DTR mice and implemented anti-TIGIT treatment in the context of the ovarian cancer model induced by ID8 cells. Our findings unveiled that a solitary administration of DT to ovarian cancer -bearing FOXP3-DTR mice induced by ID8 cells led to only a transient delay in tumor growth. In contrast, when anti-TIGIT treatment was administered to Treg-depleted mice, it yielded significant and sustained tumor regression (see Fig. 5). Consequently, our study underscores the dependence of the protective effect of anti-TIGIT treatment in inhibiting ovarian cancer growth on the presence of $Foxp3^+$ Tregs.

Discussion

Immunotherapeutic approaches, predominantly centered around ICIs, have not met the anticipated efficacy in ovarian cancer immunotherapy. As a result, some have referred to HGSOC as one of the most "immunologically cold" tumors [24]. This shortfall is attributed to the low immune cell infiltration within the tumor microenvironment of ovarian cancer, compounded by its substantial heterogeneity. In this study, we delved into the role of $TIGIT^+$ $CD4^+$ Tregs in an ovarian cancer mouse model. Our findings revealed a significant increase in $TIGIT^+Foxp3^+CD4^+$ T cells in the spleen and ascites of ovarian cancer mice, concomitant with the increase of PD-1 expression on $CD8^+$ T cells. Treatment with TIGIT monoclonal antibodies in ovarian cancer mice depended on the presence of $CD4^+$ Tregs. Therefore, TIGIT primarily exerts its inhibitory effect on the cytotoxic activity of $CD8^+$ T cells in ovarian cancer tumor cells through $CD4^+$ Tregs, ultimately impacting the progression and development of ovarian cancer.

The management of HGSOC continues to present a formidable challenge. Despite persistent correlations between immune cell infiltration and prognosis, immunotherapy for this condition has fallen short of the anticipated results [25]. Currently, therapeutic approaches for HGSOC encompass not only tailored immunotherapy targeting its heterogeneity [26] but also primarily entail combining chemotherapy with multi-targeted

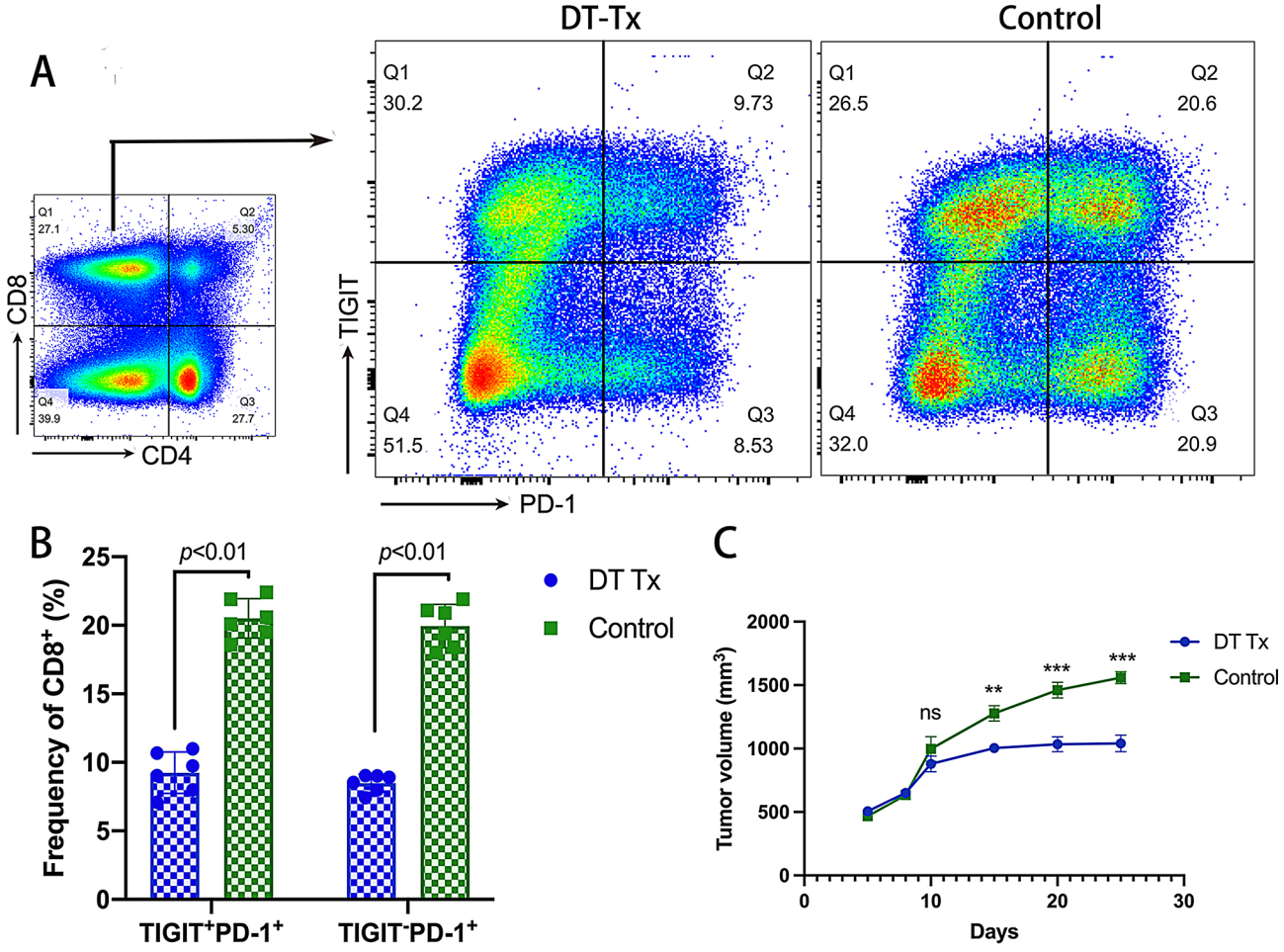

Fig. 4 Profound Alterations in expression of PD-1 on $CD8^+$ T Cell Accumulation within the Tumor Microenvironment upon $Foxp3^+$ T Cell Depletion. In this experiment, DEREG mice (six individuals per group) were injected intraperitoneally with 1 µg DT or PBS 24 h before 1×10^6 ID8 cells injection. Subsequently, 1 µg DT was administered on day 7 following tumor implantation. Control mice were treated with PBS injection. (A and B) On day 14 post DT or PBS injection, we sacrificed tumor-bearing mice that had received either PBS or DT treatment. Tumor-infiltrating lymphocytes were isolated and analyzed via FACS. The frequencies of $CD8^+TIGIT^+PD\text{-}1^+$ (9.248 ± 1.518 vs. 20.52 ± 1.439, $p < 0.01$) and $CD8^+TIGIT^-PD\text{-}1^+$ (8.482 ± 0.6521 vs. 19.95 ± 1.583, $p < 0.01$) tumor-infiltrating lymphocytes were calculated, comparing PBS control with DT-treated tumor-bearing mice. (C) The impact of $Foxp3^+$ Tregs depletion on tumor growth is depicted (Mean ± SD, $n = 4$), $p = 0.1502$ on day 10, $p = 0.0018$ on day 15, $p = 0.001$ on day 20, $p = 0.0004$ on day 25. All data were collected from three independent experiments, and the results are presented as means ± standard deviation

immunotherapy, along with immunotherapeutic interventions directed at specific cell subpopulations or broader molecular targets. Recent research has uncovered that interferon ε, with distinct activity in late-stage ovarian cancer models compared to other Type I IFNs, acts as an intrinsic tumor suppressor [27]. It represents a promising new molecular target for ovarian cancer treatment. Additionally, tissue-resident memory T cells (TRM), a specific cell subpopulation, have shown potential in both understanding the onset of ovarian cancer and its targeted intervention research [28].

In addition to TRM, Tregs represent another pivotal and specific cell subpopulation for targeted interventions in ovarian cancer [29, 30]. The immunosuppressive impact of Tregs within the tumor microenvironment serves as a substantial impediment to the optimal success of ovarian cancer immunotherapy [31]. Recent research suggests that the modulation of Tregs' glucose metabolism, possibly through Toll-like receptor 8 (TLR8), offers a promising avenue to enhance the immune landscape in ovarian cancer [30]. Furthermore, investigations have demonstrated the potential benefits of targeting Tregs in combination with chemotherapy and other therapeutic modalities for the management of ovarian cancer [29].

Immunotherapy with immune checkpoint inhibitors (ICIs) stands as a pivotal approach in current cancer treatment. Nevertheless, only a minority of ovarian cancer patients, approximately 10-15%, respond to ICI-based therapies. The resistance of ovarian cancer results from multifaceted factors, encompassing the tumor's heterogeneity, low density of tumor-infiltrating lymphocytes (TILs), non-cellular and cellular interactions

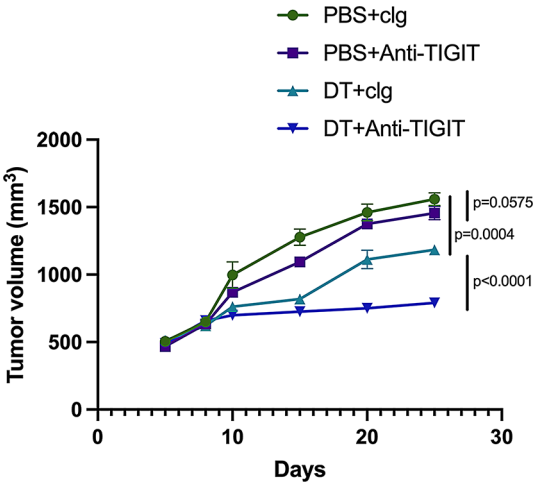

Fig. 5 Effects of Foxp3$^+$ T cells depletion and anti-TIGIT antibodies on tumor growth. ID8 cells (1×10^6) were injected i.p. in mice expressing the DTR under the control of the Foxp3 promoter (Foxp3-DTR mice) and either 1 µg DT or PBS was injected on day 12 post-tumor implantation. The anti-TIGIT mAb (clone 1B4) (100 µg) or an isotype-matched control antibody (clg) (Ultra-LEAF™ Purified Mouse IgG1, κ Isotype Ctrl Antibody, Catalog #401414, BioLegend, San Diego, CA) or with anti-TIGIT mAb (absolute IgG1 antibody, clone 1B4, Catalog #Ab01258, BioLegend, San Diego, CA) was given every 4 days from day 12 to day 24 post-tumor implantation. Tumor sizes are represented as means ± standard deviation, PBS + clg vs. PBS + Anti-TIGIT, $p=0.0877$ on day 10, $p=0.0075$ on day 15, $p=0.1078$ on day 20, $p=0.0575$ on day 25; PBS + clg vs. DT + clg, $p=0.0170$ on day 10, $p=0.0002$ on day 15, $p=0.0029$ on day 20, $p=0.0004$ on day 25; DT + clg vs. DT + Anti-TIGIT, $p=0.0408$ on day 10, $p=0.0012$ on day 15, $p=0.0009$ on day 20, $p<0.0001$ on day 25. Experiments have been repeated twice. statistical differences were calculated by Mann-Whitney analyses at the indicated time points

within the tumor microenvironment (TME), and the intricate microRNA networks regulating immune checkpoint pathways [32]. Notably, TIGIT exhibits substantial expression in malignant ascites lymphocytes and peripheral blood lymphocytes of clinical ovarian cancer patients [33], yet single-target TIGIT therapy has demonstrated suboptimal performance in ovarian cancer. CD226 is a target of TIGIT in the immune check points. A high TIGIT/CD226 ratio within Tregs is associated with elevated Treg frequencies in ovarian cancer and it predicts a less favorable clinical outcome following immune checkpoint blockade [34]. Recent research lends support to the rational combination of FAK and TIGIT targeting as an immunotherapeutic approach for treating HGSOC [19]. This study also uncovers that dual targeting of regulatory T cells and TIGIT significantly enhances CD8 T cell immune activity and boosts the survival rate of ovarian cancer mice, offering valuable insights into precise, cell-specific interventions targeting immune checkpoint molecules, exemplified by TIGIT.

Our investigation into the role of TIGIT$^+$CD4$^+$ Tregs in an ovarian cancer mouse model underscores the intricate relationship between immune cells and tumor progression. We observed a substantial increase in TIGIT$^+$CD4$^+$ Tregs in both the spleen and ascites of ovarian cancer -bearing mice. This finding highlights the accumulation of a specific subset of Tregs associated with the tumor and ascitic fluid.

Moreover, our study demonstrated that the presence of TIGIT$^+$CD4$^+$ Tregs correlates with the expression of PD-1 on CD8$^+$ T cells. This observation suggests that TIGIT$^+$CD4$^+$ Tregs may play a pivotal role in modulating the immune response within the ovarian cancer microenvironment. The dependency of TIGIT monoclonal antibody efficacy on the presence of CD4$^+$ Tregs further supports this hypothesis.

These findings provide a critical understanding of how TIGIT$^+$CD4$^+$ Tregs contribute to immune evasion in ovarian cancer. The interactions between these regulatory T cells and CD8$^+$ T cells highlight a potential mechanism through which TIGIT impairs anti-tumor immunity. This mechanism may partly explain the limited success of current immunotherapeutic approaches in treating ovarian cancer.

Future research should focus on elucidating the precise molecular pathways through which TIGIT$^+$CD4$^+$ Tregs modulate CD8$^+$ T cell activity and exploring combination strategies that target both TIGIT$^+$CD4$^+$ Tregs and other immune checkpoint pathways. Such approaches may enhance the efficacy of immunotherapies in ovarian cancer and potentially overcome the challenges associated with its immunologically cold nature.

Our study has certain limitations. Firstly, the ovarian cancer model we employed, ID8 cells, may not fully replicate the clinical heterogeneity seen in a wide spectrum of ovarian cancer patients. Secondly, we employed the 1B4 monoclonal TIGIT antibody, which exerts its function by competitively binding to TIGIT, preventing the interaction between CD155 and TIGIT. The 1B4 monoclonal antibody may potentially reduce the levels of IL-10 in CD4$^+$ regulatory T cells but does not deplete TIGIT$^+$ cells [20]. Future investigations may require the use of TIGIT gene knockout models or additional antibodies of diverse types to validate the role of TIGIT. Thirdly, while we have demonstrated the inhibitory effect of dual targeting TIGIT and Tregs on mouse ovarian cancer growth, we have not conducted an immune status assessment of the mice following this treatment. We aim to undertake further research in the future to delve into the influence on immune status and the underlying molecular mechanisms. Lastly, we only assessed the expression of PD-1 and TIGIT in CD8$^+$ T cells, without examining other molecules related to their immune function, which does not fully reflect the exhaustion status of CD8$^+$ T cells. Additionally, we did not evaluate the cytotoxic function of CD8$^+$ T cells. These aspects will be addressed in detail in future studies.

Conclusion

The immunotherapy targeting, represented by ICIs, has not demonstrated significant efficacy in the treatment of ovarian cancer. Our research suggests that combining multi-targeted approaches, building upon the existing ICIs foundation, may provide a turning point in immunotherapy for ovarian cancer. Future research in ovarian cancer immunotherapy is leaning towards a strategy that combines multiple targets, specific cell-type immunotherapies, and complementary chemotherapy. Our research has demonstrated that dual targeting of Tregs and TIGIT effectively retards tumor growth in mouse ovarian cancer model, laying the groundwork for the clinical application of immune checkpoint combination therapies, with TIGIT at the forefront.

Supplementary Information

The online version contains supplementary material available at https://doi.org/10.1186/s13048-024-01578-y.

Supplementary Material 1

Author contributions

This study was designed and mainly conducted by FC. YX contributed to the design of the study and written the manuscript. ND and LT helped with experiments and the revision of the manuscript. XL assisted in performing additional experiments and contributed to manuscript revisions. All authors participated in the review and revision of the paper. All authors reviewed and approved the final manuscript.

Funding

This work was supported by the Science and Technology Fund of Tianjin Municipal Education Commission (grant number: 2021KJ231).

Data availability

No datasets were generated or analysed during the current study.

Declarations

Ethical approval

All experimental protocols utilizing animals were conducted with approval by Tianjin Medical University's ethics committee.

Clinical trial number

Not applicable.

Competing interests

The authors declare no competing interests.

Received: 25 August 2024 / Accepted: 9 December 2024
Published online: 20 December 2024

References

1. Siegel RL, Giaquinto AN, Jemal A. Cancer statistics, 2024. CA Cancer J Clin. 2024;74(1):12–49.
2. Kuroki L, Guntupalli SR. Treatment of epithelial ovarian cancer. BMJ. 2020;371:m3773.
3. Patch AM, Christie EL, Etemadmoghadam D, Garsed DW, George J, Fereday S, Nones K, Cowin P, Alsop K, Bailey PJ, et al. Whole-genome characterization of chemoresistant ovarian cancer. Nature. 2015;521(7553):489–94.
4. Lin CN, Liang YL, Tsai HF, Wu PY, Huang LY, Lin YH, Kang CY, Yao CL, Shen MR, Hsu KF. Adipocyte pyroptosis occurs in omental tumor microenvironment and is associated with chemoresistance of ovarian cancer. J Biomed Sci. 2024;31(1):62.
5. Gambelli A, Nespolo A, Rampioni Vinciguerra GL, Pivetta E, Pellarin I, Nicoloso MS, Scapin C, Stefenatti L, Segatto I, Favero A, et al. Platinum-induced upregulation of ITGA6 promotes chemoresistance and spreading in ovarian cancer. EMBO Mol Med. 2024;16(5):1162–92.
6. Kaur K, Sanghu J, Memarzadeh S, Jewett A. Exploring the Potential of Natural Killer Cell-Based Immunotherapy in Targeting High-Grade Serous Ovarian Carcinomas. Vaccines (Basel) 2024, 12(6).
7. Balan D, Kampan NC, Plebanski M, Abd Aziz NH. Unlocking ovarian cancer heterogeneity: advancing immunotherapy through single-cell transcriptomics. Front Oncol. 2024;14:1388663.
8. Deng M, Tang F, Chang X, Liu P, Ji X, Hao M, Wang Y, Yang R, Ma Q, Zhang Y, Miao J. Immunotherapy for Ovarian Cancer: Disappointing or Promising? Mol Pharm. 2024;21(2):454–66.
9. Vazquez-Garcia I, Uhlitz F, Ceglia N, Lim JLP, Wu M, Mohibullah N, Niyazov J, Ruiz AEB, Boehm KM, Bojilova V, et al. Ovarian cancer mutational processes drive site-specific immune evasion. Nature. 2022;612(7941):778–86.
10. Curiel TJ, Coukos G, Zou L, Alvarez X, Cheng P, Mottram P, Evdemon-Hogan M, Conejo-Garcia JR, Zhang L, Burow M, et al. Specific recruitment of regulatory T cells in ovarian carcinoma fosters immune privilege and predicts reduced survival. Nat Med. 2004;10(9):942–9.
11. Sato S, Matsushita H, Shintani D, Kobayashi Y, Fujieda N, Yabuno A, Nishikawa T, Fujiwara K, Kakimi K, Hasegawa K. Association between effector-type regulatory T cells and immune checkpoint expression on CD8(+) T cells in malignant ascites from epithelial ovarian cancer. BMC Cancer. 2022;22(1):437.
12. Wu M, Chen X, Lou J, Zhang S, Zhang X, Huang L, Sun R, Huang P, Pan S, Wang F. Changes in regulatory T cells in patients with ovarian cancer undergoing surgery: Preliminary results. Int Immunopharmacol. 2017;47:244–50.
13. Erfani N, Hamedi-Shahraki M, Rezaeifard S, Haghshenas M, Rasouli M, Samsami Dehaghani A. FoxP3 + regulatory T cells in peripheral blood of patients with epithelial ovarian cancer. Iran J Immunol. 2014;11(2):105–12.
14. Brtnicky T, Fialova A, Lastovicka J, Rob L, Spisek R. Clinical relevance of regulatory T cells monitoring in the peripheral blood of ovarian cancer patients. Hum Immunol. 2015;76(2–3):187–91.
15. Toker A, Nguyen LT, Stone SC, Yang SYC, Katz SR, Shaw PA, Clarke BA, Ghazarian D, Al-Habeeb A, Easson A, et al. Regulatory T Cells in Ovarian Cancer Are Characterized by a Highly Activated Phenotype Distinct from that in Melanoma. Clin cancer research: official J Am Association Cancer Res. 2018;24(22):5685–96.
16. Manieri NA, Chiang EY, Grogan JL. TIGIT: A Key Inhibitor of the Cancer Immunity Cycle. Trends Immunol. 2017;38(1):20–8.
17. Westergaard MCW, Milne K, Pedersen M, Hasselager T, Olsen LR, Anglesio MS, Borch TH, Kennedy M, Briggs G, Ledoux S et al. Changes in the Tumor Immune Microenvironment during Disease Progression in Patients with Ovarian Cancer. Cancers (Basel) 2020, 12(12).
18. Chen F, Xu Y, Chen Y, Shan S. TIGIT enhances CD4(+) regulatory T-cell response and mediates immune suppression in a murine ovarian cancer model. Cancer Med. 2020;9(10):3584–91.
19. Ozmadenci D, Shankara Narayanan JS, Andrew J, Ojalill M, Barrie AM, Jiang S, Iyer S, Chen XL, Rose M, Estrada V, et al. Tumor FAK orchestrates immunosuppression in ovarian cancer via the CD155/TIGIT axis. Proc Natl Acad Sci U S A. 2022;119(17):e2117065119.
20. Dixon KO, Schorer M, Nevin J, Etminan Y, Amoozgar Z, Kondo T, Kurtulus S, Kassam N, Sobel RA, Fukumura D, et al. Functional Anti-TIGIT Antibodies Regulate Development of Autoimmunity and Antitumor Immunity. J Immunol. 2018;200(8):3000–7.
21. Lahl K, Loddenkemper C, Drouin C, Freyer J, Arnason J, Eberl G, Hamann A, Wagner H, Huehn J, Sparwasser T. Selective depletion of Foxp3 + regulatory T cells induces a scurfy-like disease. J Exp Med. 2007;204(1):57–63.
22. Wang J, Wu Q, Wang Y, Xiang L, Feng J, Zhou Z, Fu Q, Zhang L. Collagenase-loaded pH-sensitive nanocarriers efficiently remodeled tumor stroma matrixes and improved the enrichment of nanomedicines. Nanoscale. 2021;13(20):9402–14.
23. Tiemessen MM, Jagger AL, Evans HG, van Herwijnen MJ, John S, Taams LS. CD4 + CD25 + Foxp3 + regulatory T cells induce alternative activation of human monocytes/macrophages. Proc Natl Acad Sci U S A. 2007;104(49):19446–51.
24. Kather JN, Suarez-Carmona M, Charoentong P, Weis CA, Hirsch D, Bankhead P, Horning M, Ferber D, Kel I, Herpel E et al. Topography of cancer-associated immune cells in human solid tumors. Elife. 2018 Sep 4;7:e36967.

25. Konstantinopoulos PA, Matulonis UA. Clinical and translational advances in ovarian cancer therapy. Nat Cancer. 2023;4(9):1239–57.
26. Kandalaft LE, Dangaj Laniti D, Coukos G. Immunobiology of high-grade serous ovarian cancer: lessons for clinical translation. Nat Rev Cancer. 2022;22(11):640–56.
27. Marks ZRC, Campbell NK, Mangan NE, Vandenberg CJ, Gearing LJ, Matthews AY, Gould JA, Tate MD, Wray-McCann G, Ying L, et al. Interferon-epsilon is a tumour suppressor and restricts ovarian cancer. Nature. 2023;620(7976):1063–70.
28. Anadon CM, Yu X, Hanggi K, Biswas S, Chaurio RA, Martin A, Payne KK, Mandal G, Innamarato P, Harro CM, et al. Ovarian cancer immunogenicity is governed by a narrow subset of progenitor tissue-resident memory T cells. Cancer Cell. 2022;40(5):545–e557513.
29. Thibodeaux SR, Barnett BB, Pandeswara S, Wall SR, Hurez V, Dao V, Sun L, Daniel BJ, Brumlik MJ, Drerup J, et al. IFNalpha Augments Clinical Efficacy of Regulatory T-cell Depletion with Denileukin Diftitox in Ovarian Cancer. Clin cancer research: official J Am Association Cancer Res. 2021;27(13):3661–73.
30. Xu R, Wu M, Liu S, Shang W, Li R, Xu J, Huang L, Wang F. Glucose metabolism characteristics and TLR8-mediated metabolic control of CD4(+) Treg cells in ovarian cancer cells microenvironment. Cell Death Dis. 2021;12(1):22.
31. Cassar E, Kartikasari AER, Plebanski M. Regulatory T Cells in Ovarian Carcinogenesis and Future Therapeutic Opportunities. *Cancers (Basel)* 2022, 14(22).
32. Pawlowska A, Rekowska A, Kurylo W, Panczyszyn A, Kotarski J, Wertel I. Current Understanding on Why Ovarian Cancer Is Resistant to Immune Checkpoint Inhibitors. Int J Mol Sci 2023, 24(13).
33. Weimer P, Wellbrock J, Sturmheit T, Oliveira-Ferrer L, Ding Y, Menzel S, Witt M, Hell L, Schmalfeldt B, Bokemeyer C et al. Tissue-Specific Expression of TIGIT, PD-1, TIM-3, and CD39 by gammadelta T Cells in Ovarian Cancer. Cells 2022, 11(6).
34. Fourcade J, Sun Z, Chauvin JM, Ka M, Davar D, Pagliano O, Wang H, Saada S, Menna C, Amin R et al. CD226 opposes TIGIT to disrupt Tregs in melanoma. JCI Insight 2018, 3(14).

Publisher's note

Terms and Conditions

Springer Nature journal content, brought to you courtesy of Springer Nature Customer Service Center GmbH (“Springer Nature”).
Springer Nature supports a reasonable amount of sharing of research papers by authors, subscribers and authorised users (“Users”), for small-scale personal, non-commercial use provided that all copyright, trade and service marks and other proprietary notices are maintained. By accessing, sharing, receiving or otherwise using the Springer Nature journal content you agree to these terms of use (“Terms”). For these purposes, Springer Nature considers academic use (by researchers and students) to be non-commercial.
These Terms are supplementary and will apply in addition to any applicable website terms and conditions, a relevant site licence or a personal subscription. These Terms will prevail over any conflict or ambiguity with regards to the relevant terms, a site licence or a personal subscription (to the extent of the conflict or ambiguity only). For Creative Commons-licensed articles, the terms of the Creative Commons license used will apply.
We collect and use personal data to provide access to the Springer Nature journal content. We may also use these personal data internally within ResearchGate and Springer Nature and as agreed share it, in an anonymised way, for purposes of tracking, analysis and reporting. We will not otherwise disclose your personal data outside the ResearchGate or the Springer Nature group of companies unless we have your permission as detailed in the Privacy Policy.
While Users may use the Springer Nature journal content for small scale, personal non-commercial use, it is important to note that Users may not:

1. use such content for the purpose of providing other users with access on a regular or large scale basis or as a means to circumvent access control;
2. use such content where to do so would be considered a criminal or statutory offence in any jurisdiction, or gives rise to civil liability, or is otherwise unlawful;
3. falsely or misleadingly imply or suggest endorsement, approval , sponsorship, or association unless explicitly agreed to by Springer Nature in writing;
4. use bots or other automated methods to access the content or redirect messages
5. override any security feature or exclusionary protocol; or
6. share the content in order to create substitute for Springer Nature products or services or a systematic database of Springer Nature journal content.

In line with the restriction against commercial use, Springer Nature does not permit the creation of a product or service that creates revenue, royalties, rent or income from our content or its inclusion as part of a paid for service or for other commercial gain. Springer Nature journal content cannot be used for inter-library loans and librarians may not upload Springer Nature journal content on a large scale into their, or any other, institutional repository.
These terms of use are reviewed regularly and may be amended at any time. Springer Nature is not obligated to publish any information or content on this website and may remove it or features or functionality at our sole discretion, at any time with or without notice. Springer Nature may revoke this licence to you at any time and remove access to any copies of the Springer Nature journal content which have been saved.
To the fullest extent permitted by law, Springer Nature makes no warranties, representations or guarantees to Users, either express or implied with respect to the Springer nature journal content and all parties disclaim and waive any implied warranties or warranties imposed by law, including merchantability or fitness for any particular purpose.
Please note that these rights do not automatically extend to content, data or other material published by Springer Nature that may be licensed from third parties.
If you would like to use or distribute our Springer Nature journal content to a wider audience or on a regular basis or in any other manner not expressly permitted by these Terms, please contact Springer Nature at

onlineservice@springernature.com